Experimental verification of ultimate bending strength of glulam-steel hybrid beam

KISS Lajos*, USUKI Seizo**, GOTOU Humihiko***

* M.Sc., Ph.D. student, Dept. of Civil Eng., Akita University, 1-1 Tegata, Gakuen-machi, Akita 010-8502
**Dr. Eng., Professor, Dept. of Civil Eng., Akita University, 1-1 Tegata, Gakuen-machi, Akita 010-8502
***Dr. Eng., Assistant Prof., Dept. of Civil Eng., Akita University, 1-1 Tegata, Gakuen-machi, Akita 010-8502

Nowadays several long-span timber bridges are built worldwide, as a result of using hybrid structures, combining glued laminated timber with steel, concrete or FRP. The authors proposed the design of a glulam-steel hybrid bridge, with the intention of making timber bridge a more available option for short and medium span bridges. A bridge model was tested to investigate the bending capacity of such hybrid structures and validate the composite beam theory used by the authors to design them. The tested beam is composed of an orthotropic steel deck, attached to a double glulam beam, having rectangular cross sections. The beams are stiffened by two, vertically inserted, glued-in steel plates, having different size at the upper and lower surface. The deck is connected to the beams through the upper inserted steel plates, which also act as shear connectors. Comparing the experimental results to the theoretical ones proved the ability of the composite beam theory to describe the structural behavior of the tested model, however slightly underestimating the ultimate bending strength of the glulam-steel hybrid beam.

Key Words: glulam, orthotropic steel deck, composite beam theory, bending strength

1. Introduction

In recent years several long-span timber bridges were built worldwide, as a result of combining engineered wood material with traditional structural materials, e.g. steel or concrete or newly developed ones[1]. In the case of such hybrid bridges a frequently used technique is the King post truss structure, which is traditionally used for timber bridges. This type of truss makes full advantage of the high compressive strength of timber (the same can be said for Howe truss timber bridges). In the followings three King post truss type timber bridges are briefly presented.

One of the latest examples is Karikobozu bridge, built in Miyazaki Prefecture, Japan in 2003. The glued laminated timber main girders of this bridge are reinforced with prestressed steel rods, while the main deck is a prestressed timber one. The longest span of this bridge is 48.2 m and today it is the world's largest span[2].

Another example is the widely known Vihantasalmi bridge of Finland, completed in 1999. Here, a reinforced concrete deck slab and the glulam main girders are joined into a composite structure with steel dowels. Having three longest spans of 42.0 m, this bridge is now the world's largest timber bridge[3].

The first similar bridge in Japan was the Bochu bridge, built in Akita Prefecture, in 2001. In this case, the glulam main girders are reinforced with vertically inserted steel plates at the top and bottom surfaces. An orthotropic steel deck forms a hybrid structure with the girder, being welded to the upper inserted reinforcement. The Bochu bridge has a length of 55.0 m with two continuous spans. For bridges of this scale, this type of hybrid solution is preferred against the previous two examples, because its simple structure is easier to design and build[4),5].

One condition to make this glulam-steel hybrid bridge structure more available and familiar for clients and bridge designers is to develop a comprehensible design method. The authors proposed the use of composite beam theory as a simple, but reliable way of design for this type of bridge. In order to validate the adaptability of this theory for the hybrid structure considered, experimental verification was necessary.

The above reason determined the authors to prepare a reduced scale model of a glued laminated timber-orthotropic steel deck hybrid beam bridge. This paper presents the three-point bending test of this model. Due to the large size of the specimen, half-analysis modeling was considered. The test was conducted in the structural testing laboratory of the Institute of Wood Technology, Akita Prefectural University, situated in Noshiro City, Japan. The experimental ultimate bending strength was investigated and compared to the one predicted by the composite beam theory.

2. Bridge Conception

A very important aspect in the design of beam bridges is the ratio of beam height versus span length. Choosing this ratio to be comparable to ratios of other types of bridges helps making the timber bridge a viable option for bridge building. The authors proposed a glued laminated timber and orthotropic steel deck hybrid beam bridge structure, for short and medium span bridges, having the height-span ratio h/l = 1/16. The cross section of bridge prototype is shown in Fig.1. As a comparison, in the case of reinforced concrete beam bridges this ratio is h/l = 1/16, for prestressed concrete beam bridges it will be h/l = 1/24 and for steel plate girder bridges h/l = 1/15－1/20.

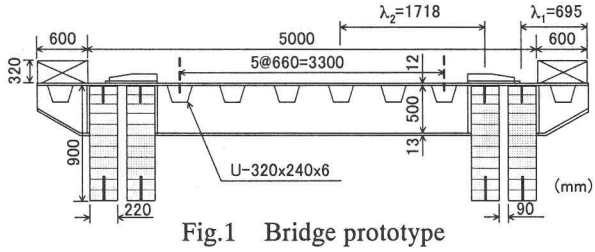

Fig.1 Bridge prototype

To investigate the behavior of this kind of hybrid structure, a reduced scale model was subjected to bending test[7]. Due to the large size of this 1/3 model, the authors chose a half-analysis modeling approach. Geometry of the specimen is shown in Fig.2 and Fig.3. The tested structure consists of an orthotropic steel deck, attached to a double glulam beam. The orthotropic steel deck plate has a total length of 5200 mm (span is 5000 mm), a width of 1033 mm and a thickness of 4.5 mm. The deck plate is stiffened by four U-shaped longitudinal ribs and seven ⊥-shaped transverse ribs, the latter being arranged with an interval of 833 mm. The steel deck acts as the top flange of the double beam, having rectangular cross sections.

The beams are stiffened by two, vertically inserted, glued-in ribbed steel plates, having different size at the upper and lower surface. The size of the upper ribbed plate is 3x44 mm, while the lower one has a cross section of 6x65 mm (see Fig.3). After removing mill scale by sandblasting, these steel plates are bonded by E6264D, an epoxy resin designed for steel-timber hybrid bridges. The deck is connected to the beams through the upper inserted steel plates. These are welded through the whole length to the bottom surface of the steel deck plate and act as shear connectors. The role of the glued-in ribbed steel plates on the lower surface of the beams is to compensate the longitudinal axial strength of beams.

The beam width of a single beam varies from 73.5 mm to 113 mm at near beam ends, in order to overcome shear forces developed by reactive forces on the support[8]. This variation takes place on a length of 400 mm, taking a gradient of 1:10, since no other specification exists for it. The length of widened beam portion is 985 mm. The beam depth remains constant, being equal to 300 mm (see Fig.2).

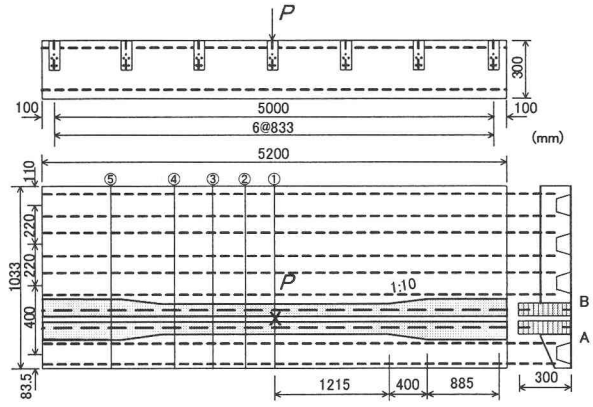

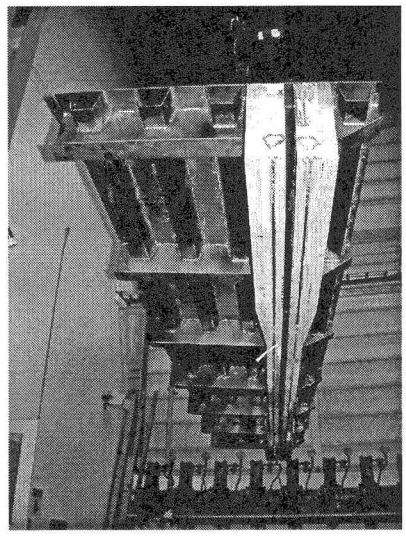

Fig.2 Bridge model: strain gage location, side and plan view

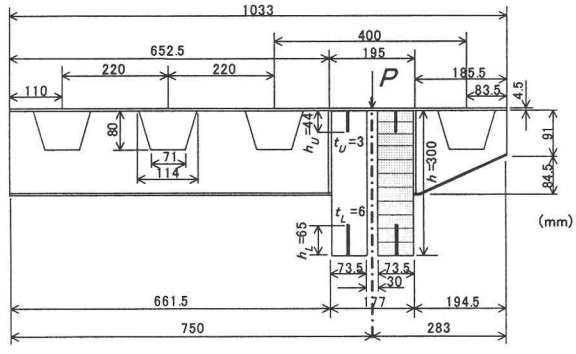

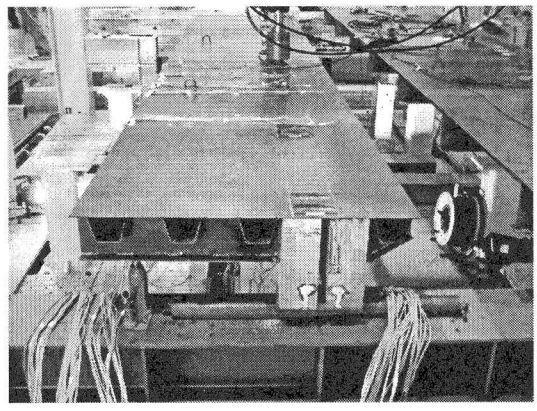

Fig.3 Bridge model: cross section

3. Composite Beam Theory

3.1 Material Properties

Three-point bending tests of glulam beam-orthotropic steel deck hybrid bridge model were conducted in the structural testing laboratory of the Institute of Wood Technology, Akita Prefectural University, situated in Noshiro City, Japan. A load-controlled testing machine loaded the simply supported hybrid beam. Two bridge models were tested, however in this paper only one is presented in detail.

The strength grade of Douglas fir glulam used for the bridge model was E120-F330. To verify the actual parallel-to-grain modulus of elasticity as well as the bending moment capacity of the timber material, twelve specimens were tested. These pieces were cut out from the double glulam beam of the hybrid model, after the failure test was over. The cross section of these small beams was 45x65 mm, having a span length of 1300 mm.

The statistical analysis of the test data resulted in higher bending capacity and smaller modulus of elasticity compared to the nominal values. Test data of bending moment capacity fit a 2-parameter Weibull distribution. The non-parametric, 5% tolerance limit with 75% confidence level is $\sigma_{Y,W} = 47$ MPa. The allowable bending strength is equal to 1/3 of the bending strength, i.e. $\sigma_{A,W} = \sigma_{Y,W}/3 = 16$ MPa. In the case of the bending modulus, the lower 95% confidence limit on the mean value of the Young's modulus was used to establish the value of $E_W = 10.4$ GPa. The shear modulus was taken as $G_W = 648$ MPa, determined from an earlier bending test.

The steel material used for the inserted steel plates as well for the orthotropic steel deck is SMA490W. The yield strength of this material is $\sigma_{Y,S} = 353$ MPa, the allowable strength is $\sigma_{A,S} = 206$ MPa, while the bending modulus is $E_S = 200$ GPa.

3.2 Theoretical Bending Moments

The concept of transformed section was applied by the authors[9]. This makes the calculation of composite cross section properties possible. Using the ratio of moduli of elasticity, all steel components are converted into an equivalent wood area:

$$n = \frac{E_S}{E_W} = \frac{200}{10.4} = 19 \tag{1}$$

The authors used the composite beam theory to determine specific bending moments and the corresponding loads, assuming that the steel deck, the inserted steel plates and the double glulam beam work together, i.e. constitute a composite beam. These specific moments are based on the following theoretical assumptions.

The yield moment M_Y is the bending moment for which yielding of lower inserted steel plate starts. At this phase, the tensile stress of the steel plate reaches the yield strength of steel, i.e. $\sigma_x = \sigma_{Y,S} = 353$ MPa. The plastic moment M_P is supposed to occur when at mid-span, the cross section of the lower inserted steel plate is in fully plastic state. Determination of the ultimate moment M_U is based on the assumption that failure of the composite beam takes place when the tensile stress in the outer fibers of the double glulam beam reaches the modulus of rupture of the timber material, i.e. when $\sigma_x = \sigma_{Y,W} = 47$ MPa.

Theoretical expressions of these bending moments are presented below:

$$M_Y = \frac{\sigma_{Y,S}}{\frac{h}{2} - e_Y}\left[\bar{I}_S + \frac{1}{n}\bar{I}_W - e_Y^2\left(A_S + \frac{1}{n}A_W\right)\right] \tag{2}$$

$$M_P = \frac{\sigma_{Y,S}}{\frac{h}{2} - h_L - e_P}\left[\bar{I}_S + \bar{I}_P + \frac{1}{n}\bar{I}_W - e_P^2\left(A_S + A_P + \frac{1}{n}A_W\right)\right] \tag{3}$$

$$M_U = \frac{\sigma_{Y,W}}{\frac{h}{2} - e_U}\left[n\bar{I}_S + m\bar{I}_P + \bar{I}_W - e_U^2\left(nA_S + mA_P + A_W\right)\right] \tag{4}$$

$$m = \frac{\sigma_{Y,S}}{\sigma_{Y,W}} = \frac{353}{47} = 7.5 \tag{5}$$

where e_Y, e_P and e_U are the coordinates from the neutral axis of double beam to the neutral axis of the composite beam for yield, plastic and ultimate bending moments, respectively; A_S is the cross section area of steel being in elastic state, while A_P is the area of steel being in plastic state; $\bar{I}_S$ and $\bar{I}_P$ are the moments of inertia for the previous steel areas, calculated with respect to the neutral axis of double beam. Numerical values of these variable quantities are tabulated in Table2. The remaining quantities are constants and they are the timber area $A_W = 430.6$ cm^2 and the elastic moment of inertia of timber $\bar{I}_W = 31.5 \times 10^3$ cm^4.

According to the loading scheme applied for the bending test, the following simple expression was used to determine the load values for each specific bending moment:

$$P_i = \frac{2M_i}{\mu L} \tag{6}$$

where subscript i stands for Y, P, U, respectively.

Calculated values of equations (2), (3) and (4) and the corresponding loads from equation (6) are shown in Table 1.

Table1 Calculated bending moments and loads

Case	M_i & P_i		Unit	P_i/P_A
Allowable	M_A	75.9	kN·m	1
	P_A	60.7	kN	
Yield	M_Y	130.1	kN·m	1.7
	P_Y	104.1	kN	
Plastic	M_P	166.9	kN·m	2.2
	P_P	133.5	kN	
Ultimate	M_U	249.9	kN·m	3.3
	P_U	199.9	kN	

3.3 Theoretical Deflections

The method of virtual work, or sometimes referred to as the unit-load method, is one of the several techniques available that can be used to solve for displacements and rotations at any point on a structure.

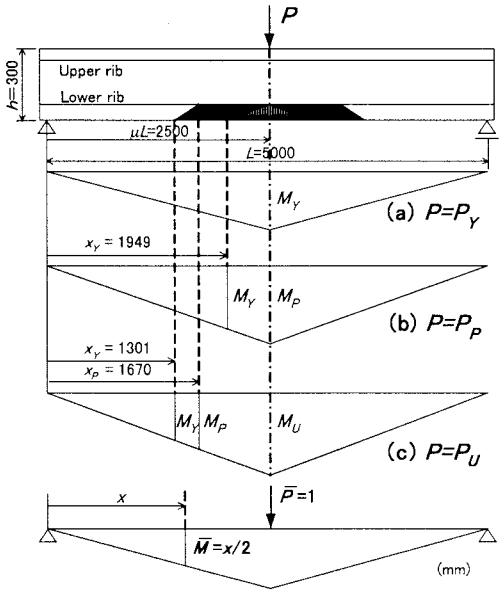

Fig.4 Loading scheme and method of virtual work

The mid-span deflections for each specific bending moment are expressed as follows:

$$\delta_Y = \frac{P_Y L^3}{48 E_W I_{V,Y}} \mu\left(3 - 4\mu^2\right) + \frac{\kappa P_Y \cdot \mu L}{2 G_W A_V} \tag{7}$$

$$\delta_P = \frac{M_P}{E_W}\left(\frac{x_Y^3}{3 I_{V,Y} \mu L} + \frac{1}{\mu L}\int_{x_Y}^{\mu L} \frac{x^2}{I_{V,P}} dx\right) + \frac{\kappa P_P \cdot \mu L}{2 G_W A_V} \tag{8}$$

$$\delta_U = \frac{M_U}{E_W}\left(\frac{x_Y^3}{3 I_{V,Y} \mu L} + \frac{1}{\mu L}\int_{x_Y}^{x_P} \frac{x^2}{I_{V,P}} dx + \frac{\mu^3 L^3 - x_P^3}{3 I_{V,U} \mu L}\right) + \frac{\kappa P_U \cdot \mu L}{2 G_W A_V} \tag{9}$$

where x_Y is the coordinate from the support to the cross section where the bending moment is $M = M_Y$, used when $M_{max} \geq M_Y$; x_P is the coordinate of cross section position where the bending moment is $M = M_P$, used when $M_{max} \geq M_P$, μL is the coordinate of cross section being under the applied load: in the case of a three-point bending test $\mu = 0.5$; $I_{V,Y}$ is the elastic moment of inertia of the composite beam, used when $M \leq M_Y$; $I_{V,P}$ is the plastic moment of inertia of the composite beam, used in the case $M_Y \leq M \leq M_P$; $I_{V,U}$ is the ultimate moment of inertia of the composite beam, used when $M_P \leq M \leq M_U$.

These quantities are variable ones. In equations (7), (8) and (9) however the following constants are also used. One of them is the equivalent cross section area of composite beam. This area is determined by equation (10) and has the value of $A_V = 1747\ cm^2$.

$$A_V = A_W + n\left(A_S + A_P\right) \tag{10}$$

The other constant is the shear factor of cross section, being equal to $\kappa = 4.32$.

The behavior of composite beam changes from elastic state to plastic state, therefore the position of neutral axis changes too: it moves from its initial position towards the compression side, i.e. towards the steel deck. As a consequence, the equivalent moment of inertia $I_{V,i}$ of the composite beam decreases as the bending moment increases (see Table2). This is the reason why in the deflection equations (7), (8), (9) the left-side member δ_M is divided into two portions when $P = P_P$ in Fig.4(b) and to three portions when $P = P_U$ in Fig.4(c), corresponding to the limit cross sections marked by M_Y, M_P and M_U.

Table2 Calculated moments of inertia

Case	e_i	A_S	A_P	I_S	I_P	$I_{V,i}$
	cm	cm^2	cm^2	$x10^3\ cm^4$	cm^4	$x10^4\ cm^4$
Yield	-8.13	69.3	0.0	13.0	0	16.19
Plastic	-8.40	61.5	7.8	11.8	992	15.18
Ultimate	-9.09				1144	13.38

Numerical values of mid-span deflections at the specific moments are presented in Table3. It can be seen that while the bending moment increases from the yield moment towards the ultimate moment, at the same time the shear effect decreases, resulting in smaller shear deflections δ_V compared to the total

Table3 Calculated deflections in mm

Case	δ_M	δ_V	$\delta_i = \delta_M + \delta_V$		δ_V / δ_i(%)
Yield	16.1	5.0	δ_Y	21.1	23.5
Plastic	21.4	6.4	δ_P	27.8	22.9
Ultimate	35.9	9.5	δ_U	45.4	21.0

deflections δ_i. The reason of this decrease can be explained using equation (9) of the ultimate deflection δ_U. The shear component contains only one variable term (the applied load), while all the other terms are constants (κ, G_W , A_V). In contrast to this, the bending component of δ_U increases due to several variables. One of these is the bending moment, which continues to increase until failure. At the same time, the equivalent second moment of inertia $I_{V,i}$ of the composite beam decreases (see Table2), this value being inverse proportional to the deflection. The smaller the coordinates x_Y and x_P become, the larger the effect of the variable $I_{V,i}$ becomes. These coordinates change due to the spreading of plastic region in the lower inserted steel plate as the moment increases. The plastic zone starts spreading from the mid-span toward the ends of the beam, until the bending moment reaches its ultimate value. This is illustrated in Fig.4(a), (b) and (c).

4. Bending Test Results

The bending test was performed to validate the theoretical assumptions the authors used when applying the composite beam theory. The most important results are presented in this chapter. Theoretical and experimental curves of the load P versus the mid-span deflection δ are reported in Fig.5. The theoretical curve was considered with and without the shear effect taken into account. One might observe the accidental coincidence of the theoretical curve without shear and the experimental curve of the deck. But more important is the fact that the theoretical curve with shear effects considered closely follows the experimental curves of members A and B of double beam. The experimental value of the maximum load, corresponding to the ultimate bending moment is $P_{U,EXP}$ = 238 kN. This value is 19% higher than P_U = 200 kN, determined by the composite beam theory. For P = 200 kN, the experimental deflections of the component beams of double glulam beam are measured as δ_A = 44.5 mm and δ_B = 46.1 mm, corresponding to glulam beam A and B, respectively (see Fig.2). These values are slightly lower and higher, respectively, than the theoretical value of δ_U = 45.4 mm (see Table3). As mentioned above, the theoretical $P-\delta$ curve (with shear effects) follows closely the behavior of beams A and B, however the applied theory fails to predict the maximum deflections of $\delta_{A,MAX}$ = 61.3 mm and $\delta_{B,MAX}$ = 64.2 mm.

The theoretical value of ultimate load and deflection is less than the experimental one due to the dispersion of low-strength timber material and the low number of test data (see 3.1).

In spite of theoretically considering a composite beam, experimental data shows a separation of load-deflection curves of deck ($\delta_{deck,MAX}$ = 53.2 mm) and glulam members of the double beam. This is due to the fact that the steel-glue-timber interaction was not sufficient during the test, i.e. the composite action between the deck and double beam failed to work in the way it was assumed.

Strain gages were installed along the depth of double glulam beam, located at the bottom of lower inserted steel plates as well as on the upper surface of orthotropic steel deck. Gages are located along line ①—⑤, line ① being at the mid-span of bending test specimen, under the applied concentrated load (see Fig.2). Also, at mid-span, bottom of U-ribs were provided with strain gages.

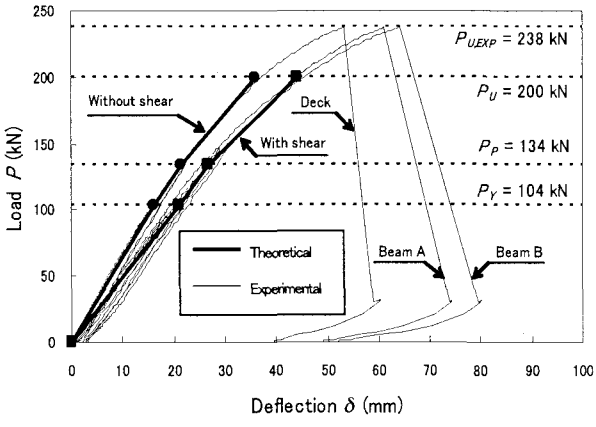

Fig.5 Theoretical and experimental curves of load versus mid-span deflection

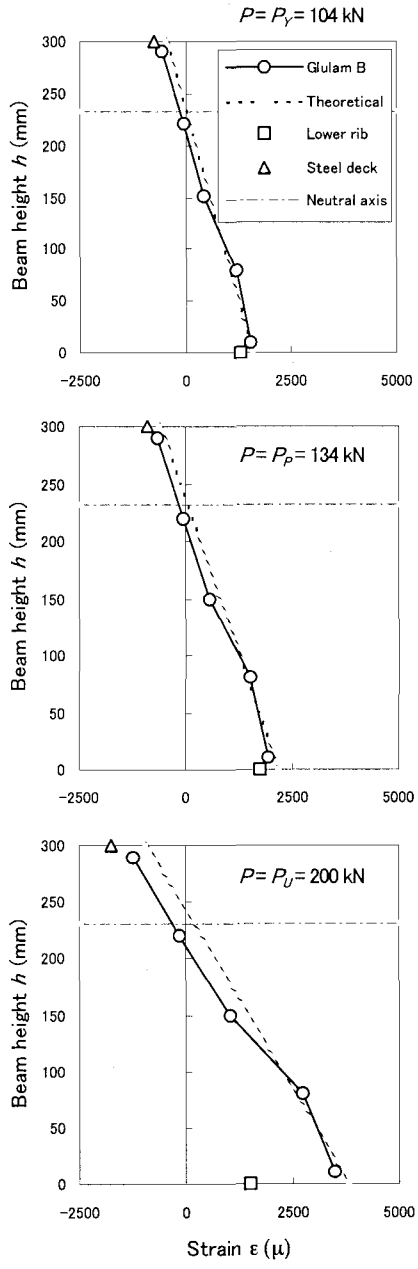

Fig.6 Strain state at specific load steps

Longitudinal strain state of some of the main composite beam components (steel deck plate, glulam beam and lower inserted steel plate) at the specific loads P_Y , P_P and P_U is presented in Fig.6. The strains included in this lateral view were measured at line ②, positioned at 306 mm from the mid-span. It can be seen that on one hand, at the upper part of the glulam beam strain values of the deck and timber are relatively close to each other. On the other hand, in the case of the ultimate load, at the lower part of the beam the strain value of the lower inserted plate and timber are separated. This is due the separation of the steel plate from the timber. Theoretical values of strain manage to closely predict the experimental values.

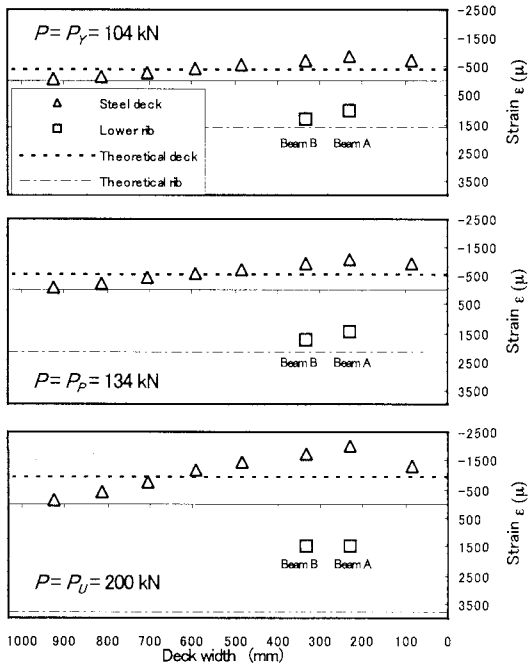

Fig.7 Deck and lower rib strain state at specific load steps

Fig.7 is a cross section view of the strain state at line ② of the steel deck plate and lower inserted steel plate at the specific loads. The strain distribution of the steel deck was assumed to be uniform, however data indicate a variable distribution in transverse direction. This is due to difficulties in restraining the symmetry edge, i.e. satisfying the symmetry condition of the model. During the test, the longitudinal symmetry edge actually behaved as a free edge. As in the case of Fig.6, for loads P_Y and P_P the experimental values of lower rib strain are close to the theoretical ones, but for P_U they are distinguishably separated.

5. Concluding Remarks

The authors proposed a glulam and orthotropic steel deck hybrid beam bridge structure for short and medium span bridges. The design of this bridge was made with the purpose of transforming timber bridge into a more competitive option for bridge designers. To help achieving this goal, the authors also developed a simple procedure to be able to determine the strength and stiffness capabilities of the proposed structure. A reduced scale bridge model was subjected to bending test in order to validate the theoretical approach.

Experimental results show the effectiveness of the applied composite beam theory in being able to predict the structural behavior of the hybrid structure. The theoretical load-deflection curve, with shear effects considered, was able to closely follow the behavior of the double glulam beam. During the test, composite action between steel-glue-timber was not sufficient enough, but the bearing capacity was still larger than the expected value.

The simple calculations provided in his paper proved to be useful for design purposes, however it slightly underestimated the ultimate bending strength of the structure. The ease of use of the composite beam theory greatly helps the work of bridge designer, but the experimental verification is made only by one bending test. Therefore to check the results obtained by the composite beam theory and presented in this paper, the authors also intend to perform a three-dimensional finite element analysis.

The 3D FEM analysis will involve difficult tasks such as taking into account the elasto-plastic behavior of the hybrid structure. This means dealing with solid and plate elements, resulting in a huge number of degrees of freedom. This analysis needs a very large stiffness matrix, requiring a high-performance computer. This is one of the reasons why the authors tried as a first attempt a simple calculation to determine the bending capacity of this type of glued laminated timber-orthotropic steel deck hybrid beam bridge structures.

References

1) Bob, L., Gruin, A., Kiss, L.: Alternative reinforcements of wooden beams, *Proceedings of IABSE Conference on Innovative Wooden Structures and Bridges*, pp.501-506, 2001

2) Hirota, T., Irie, T. and Kurushima, T., The design and plan of Karikobozu-Bridge, *Proceedings on the 2nd Symposium on Timber Bridges*, pp. 15-20, 2003 (in Japanese)

3) Rantakokko, T., Salokangas, L., Design of the Vihantasalmi Bridge, Finland, *Structural Engineering International, IABSE*, Vol.10, No.3, pp.150-152, 2000

4) Usuki, S., Atsumi, A., Sudo, S. and Iijima, Y., A new timber beam bridge with an orthotropic steel deck, *Proceedings of the 6th World Conference on Timber Engineering*, pp.8.3.3-1 - 8.3.3-7, 2000

5) Usuki, S., Sasaki, T., Honda H., Iijima Y. and Atumi A., Field experiment of a hybrid timber-steel deck roadway bridge, *Proceedings of IABSE Conference on Innovative Wooden Structures and Bridges*, pp.181-186, 2001

6) Usuki, S., Sasaki, T., Gotou, H., Kiss, L., Ultimate strength of glulam sandwich beam reinforced by inserted steel ribs, *57th JSCE Annual Meeting*, I-366, 2002 (in Japanese)

7) Kiss, L., Usuki, S., Terada, H., Gotou, H. and Fujishima, E., Glued laminated timber and orthotropic steel deck hybrid beam: ultimate bending strength, *Proceedings of the 2nd Symposium on Timber Bridges*, pp.101-106, 2003

8) Usuki, S., Sasaki, T., Atsumi, A., Sharma, M.P.: Shearing stress of longitudinal rib plate of hybrid timber beam and orthotropic steel deck, *Journal of Structural Engineering, JSCE*, Vol. 47A, pp.1221-1227, 2001 (in Japanese)

9) Usuki, S., Gotou, H. and Kiss, L., Bending capacity of glued-laminated timber stiffened with inserted steel plate, *Journal of Structural Engineering, JSCE*, Vol. 49A, pp.889-894, 2003 (in Japanese).

(Received September 12, 2003)